# HCl Yield from OH + ClO: Stratospheric Model Sensitivities and Elementary Rate Theory Calculations

**Manvendra K. Dubey,[†,§] Mark P. McGrath,[‡] Gregory P. Smith,[*,†] and F. Sherwood Rowland[‡]**

*Molecular Physics Laboratory, SRI International, Menlo Park, California 94025, and Department of Chemistry, University of California, Irvine, California 92697*

*Received: January 22, 1998; In Final Form: March 10, 1998*

Compared to measurements, atmospheric models have overestimated [ClO]/[HCl] and [$ClONO_2$]/[HCl] in the upper and middle stratosphere, respectively, and consequently have predicted lower [$O_3$] than observed. It is believed that a minor branch that produces HCl from the OH + ClO reaction can account for these discrepancies. Recent laboratory studies have indicated a 5 ± 2% yield for this channel.[1] By performing box model sensitivity analysis calculations using the output from the LLNL-2D diurnally averaged stratospheric model, we quantitatively confirm that this reaction is the most prominent contributor to the model [ClO]/[HCl] and [$ClONO_2$]/[HCl] uncertainties in the upper stratosphere and that it is most effective in increasing [$O_3$] at higher latitudes during winter. Using theoretical methods, we examine the OH + ClO reaction mechanism, in which an initially energized HOOCl* complex is formed that can dissociate to $HO_2$ + Cl (major) or HCl + $O_2(^1\Delta)$ (minor) products, redissociate to reactants, or be collisionally stabilized. Multichannel RRKM calculations guided by ab initio electronic structure calculations and the available kinetic data are presented. We show that the four-center transition state (TS3) for HCl production must lie at least 2 kcal/mol below the reactants for the HCl yield to exceed 5%. Our ab initio relative energy of −2.3 ± 3 kcal/mol for TS3 demonstrates that this minor HCl channel is mechanistically feasible. We also predict small pressure, temperature, and H/D isotopic dependencies for the minor channel yield and insignificant rates of complex stabilization under atmospheric conditions.

## Introduction

Current stratospheric models overestimate ozone loss rates (relative to observational data) at high altitudes[2,3] and underestimate trends in column ozone losses at mid to high latitudes.[3,4] Resolution of these discrepancies is essential in order to build confidence in assessments of stratospheric ozone changes from possible future natural (e.g., volcanoes) and anthropogenic (e.g., supersonic aviation, halocarbon regulation) perturbations. Simultaneous field observations of the concentrations of several species active in ozone photochemistry serve to constrain the mechanisms and have emerged as powerful guiding tools for model development. In addition, theoretical study of the potential pathways of the relevant elementary reactions is now feasible.

Analysis of mixing ratios from satellite, balloon, and shuttle borne remote sensing instruments has revealed that models underestimate [HCl] and overestimate [$ClONO_2$], [ClO], and [HOCl] at altitudes above 24 km and therefore predict lower [$O_3$] than observed.[5−7] Model sensitivity studies show that modifying the reaction of OH with ClO, known to yield $HO_2$ and Cl as major products (1a), by proposing a minor channel that produces HCl (1b),

$$OH + ClO \rightarrow HO_2 + Cl \quad (1a)$$

$$\rightarrow HCl + O_2(^1\Delta) \quad (1b)$$

can ease this problem.[5−8] A small branching fraction (7−10%) for HCl production allows the model to simulate the observed chlorine partitioning. In addition, at high altitudes the lower ClO abundance reduces the ozone loss rates and balances it with the ozone production rates.[9] In a 2-D $O_3$ assessment model, the HCl channel increases upper stratospheric [$O_3$] while damping its seasonal amplitude, in better agreement with satellite observations.[10] In the polar sunlit stratosphere the HCl produced by (1b) would also enhance chlorine activation on polar stratospheric clouds and thus the concomitant ozone depletion.[11] The 1994 NASA evaluation (JPL-94)[12] places an upper limit of 0.14 on the branching ratio of channel 1b, based on low-pressure (<5 Torr) discharge flow measurement yields for $HO_2$ + Cl of >0.65,[13] 0.85 ± 0.2,[14] 0.86 ± 0.14,[15] and 0.98 ± 0.12.[16] The last study,[16] in which HCl was also monitored, found no evidence for the minor channel. However, a small but atmospherically significant yield of HCl could not be ruled out. In fact, a recent high-pressure (100 Torr) turbulent discharge flow study of reaction 1 using H/D isotopic labels found a 5 ± 2% yield for DCl, providing the first direct evidence for channel 1b.[1]

This paper first examines the reaction rate parameter uncertainties in the chlorine partitioning and [$O_3$] in upper stratospheric models. A direct sensitivity analysis is applied to local altitude boxes from the LLNL-2D model. Sensitivities are used to propagate rate constant errors through the model and to isolate those steps that dominate the uncertainties in the predicted concentrations. We confirm that reaction 1b is indeed the most important source of uncertainty in chlorine partitioning in the 2-D atmospheric model and quantify the extent to which other specific reactions also contribute to the uncertainty. To help confirm the viability of reaction 1b, we then develop the

* To whom correspondence should be addressed.
† SRI International.
‡ University of California, Irvine.
§ Current address: Los Alamos National Laboratory, Los Alamos, NM 87545.

S1089-5639(98)00847-0 CCC: $15.00 
Published on Web 04/14/1998

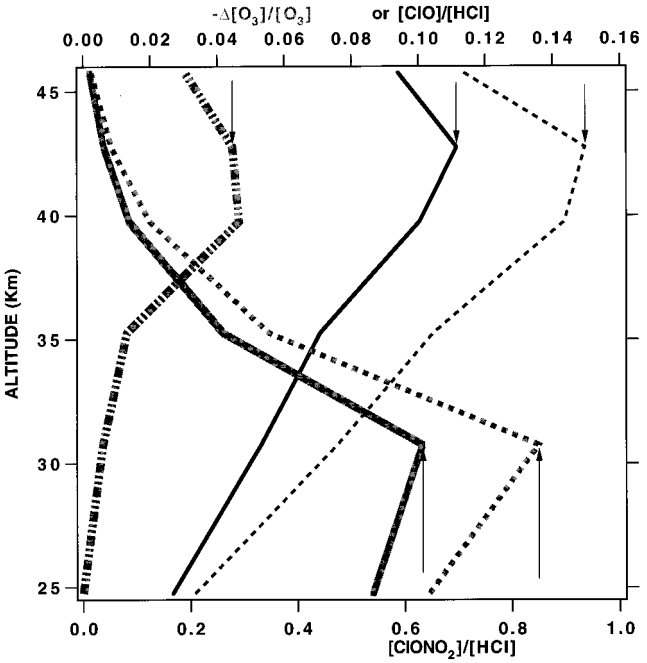


**Figure 1.** Impact of the 7% HCl branch (1b) on diurnally averaged [ClO]/[HCl] (thin black lines, arrows from upper axis), [$ClONO_2$]/[HCl] (thick lines, lower axis), and [$O_3$] as a function of altitude in the LLNL-2D model at 32°N vernal equinox. The solid lines and dashed lines are the respective model results with and without the HCl branch. Only the fractional decrease in [$O_3$] (i.e., $-\Delta[O_3]/[O_3]$) upon including the 7% HCl branch is plotted (dash dot-dot, upper axis).

elementary reaction mechanism for the OH + ClO reaction, which involves the formation, decomposition paths, and stabilization of an excited HOOCl* complex. We constrain the geometrical structures, vibrational frequencies, and energies of HOOCl and the transition states using ab initio electronic structure calculations and available kinetic and thermodynamic information. Multichannel RRKM rate theory calculations are performed to construct a relation between the HCl yield and the relative four-center transition-state energy, which is varied within the broad range suggested by our ab initio results. The predicted H/D isotope effect and temperature and pressure dependencies are discussed in light of the recent results of Molina and co-workers.[1] Finally, observed electronic barriers and isotope effects in some analogous systems are used to indirectly evaluate the plausibility of channel 1b.

## Model Sensitivity−Uncertainty Analysis of $ClO_x$, HCl, and $O_3$

To quantify the rate parameter uncertainties, we performed a local sensitivity−uncertainty analysis of the photochemistry in several altitude boxes taken from the LLNL-2D diurnally averaged, seasonally varying, chemical-radiative transport model of the stratosphere.[17] We have recently developed and applied this methodology to determine rate parameter uncertainties in the assessment of stratospheric ozone depletion caused by future supersonic aviation[18] and in the modeling of global ozone levels.[19] The JPL-94 mechanism, which includes 155 reactions and photolysis rates, was augmented to include a 7% branch to the HCl producing channel 1b in the sensitivity calculations. Our first objective was to determine the uncertainty in the LLNL-2D $O_3$ assessment model arising from omitting channel 1b. Figure 1 shows that the effect of including a 7% HCl branch on chlorine partitioning in the model, at 32°N vernal equinox, is a large reduction in model [ClO]/[HCl] at high altitudes (40 km) and [$ClONO_2$]/[HCl] at mid altitudes (30 km). This structure is similar to the instantaneous model calculations of ref 7, which were constrained by shuttle borne observations (ATLAS), although our magnitudes are smaller because of diurnal averaging. (We note that the use of diurnal averaging in the LLNL-2D model reduces concentrations of radicals such as ClO, OH, $HO_2$, and BrO to about 0.3 times their peak noon values, with a similar reduction in their radical−radical rate constants and photolysis rates.) Our analysis shows that channel 1b significantly effects chlorine partitioning in the unconstrained diurnally averaged LLNL-2D $O_3$ assessment model as well. Figure 1 also shows that a 7% yield for (1b) reduces the predicted [$O_3$] by 5% at high altitudes, with a much smaller reduction at low altitudes.

We performed a direct sensitivity−uncertainty analysis for each altitude box to sample the complete reaction rate parameter uncertainty space, using a 7% yield for (1b). The rate constants and concentrations from each box were input to the SENKIN sensitivity analysis code.[20] SENKIN integrates the time-dependent kinetics equations and also efficiently computes all species concentration derivatives with respect to all input rate parameters. This allows us to obtain a complete set of local linear sensitivity coefficients: $S_i(X) = \partial(\ln[X])/\partial(\ln k_i)$. The sensitivity of a species concentration ratio to a given rate constant $k_i$ is given by the difference in individual sensitivities, $S_i(X/Y) = S_i(X) - S_i(Y)$. A local fractional change or uncertainty in a species concentration can be predicted by the product of the relative change or error bar in the rate constant with the normalized sensitivity coefficient: $\Delta_i[X]/[X] = S_i(X)\,\delta k_i/k_i$. (In addition, the total expected kinetic error limit in model species concentration can be estimated by taking the square root of the sum of the squares of these uncertainty contributions from the individual reactions.) Here we use the JPL-94 uncertainties, with 7 ± 7% for the channel 1b branching fraction (i.e., $\delta k_{1b}/k_{1b} = 1.0$). Note that while the 7 ± 7% uncertainty range is numerically convenient and consistent with the JPL-94 recommendations, the recently measured yield of 5 ± 2% by Lipson et al.[1] should be regarded as more realistic.

Because the sensitivity coefficients are the time-dependent response of the system to infinitesimal perturbations of the rate parameters, they increase with time and converge on the time scale of the local photochemistry. We ran the SENKIN code until the sensitivities obtained were converged. Here we focus on our results at 40 and 30 km, where the largest disagreements between observations and models of chlorine partitioning occur and where channel 1b is most effective in fixing them (see Figure 1 and ref 7). Integration times of a week at 40 km and 2 months at 30 km were needed for convergence. During this time the steady-state solution to the kinetics remains close to the original starting concentrations from the 2-D model box. As mentioned above, diurnal averaging often leads to ClO concentrations and sensitivities that are smaller than their daytime values in diurnally varying models. However, the diurnally averaged model uncertainties still provide a consistent and reliable guide to the sources of potential error.

In Figure 2a, products of the sensitivity coefficients with the JPL-94 1$\sigma$ error bars identify the 11 reactions that can alter the diurnally averaged model [ClO] to [HCl] ratio by 5% or more at 40 km. The combined root-mean-square (rms) uncertainty is 62%, and the channel 1b uncertainty can alter the diurnal average ratio by 31%. While the [ClO]/[HCl] sunset observations disagree with the model by over 100% at mid latitudes, diurnal averaging should lower this discrepancy to about 30%. As expected, our quantitative analysis shows that the (1b)

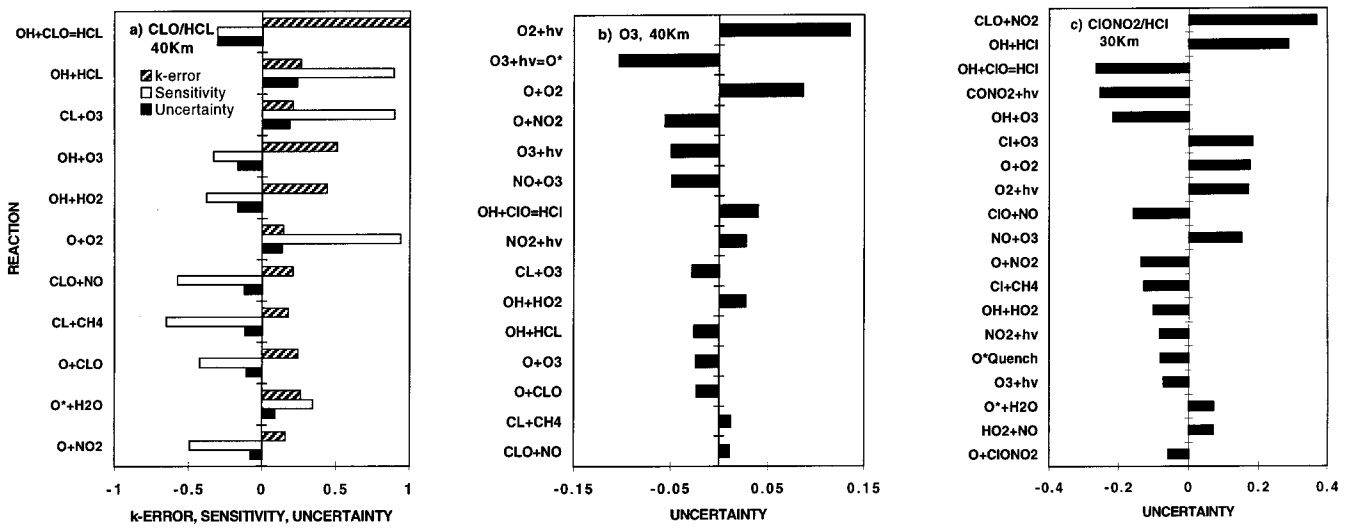


**Figure 2.** Uncertainty analysis distribution for [ClO]/[HCl] and [$O_3$] at 40 km, and [$ClONO_2$]/[HCl] at 30 km, for the LLNL-2D model at 32°N vernal equinox. The uncertainty from a particular reaction rate constant is the product of its JPL-94 1$\sigma$ error bar with its sensitivity. We retain the sign of the sensitivity in the uncertainty to show if increasing a rate constant will increase (+) or decrease (−) the particular concentration or concentration ratio.

uncertainty is the largest contributor. But errors in the other reaction rate constants identified in Figure 2a can also be responsible for some of the discrepancy. While the use of a 7% branch for (1b) can ease the previously discussed modeling discrepancies,[7] reference to Figure 2a shows further that alternative solutions must involve changing two or more of the other rate constants by substantial fractions of their error limits (e.g., both reducing OH + HCl and increasing Cl + $CH_4$ by their JPL-94 1$\sigma$ error bars). In addition, since the sensitivity of [ClO]/[HCl] to the rate constant of the Cl + $HO_2$ reaction is quite small (0.058), for this reaction to impact chlorine partitioning, the error bar for its rate constant must be significantly larger than is currently recommended.

Similar sensitivity−uncertainty analyses for diurnally averaged [$ClONO_2$]/[HCl] at 30 km reveals the 19 reactions (see Figure 2c) that can alter this ratio by 5% or more. The net rms uncertainty is 79%, with an individual contribution from channel 1b (26%) of the same order as those from ClO + $NO_2$ recombination (37%), OH + HCl (29%), $ClONO_2$ photolysis (25%), OH + $O_3$ (22%), and Cl + $O_3$ (18%). Reducing the uncertainties in these laboratory rate constants would obviously strengthen model predictions of observed [$ClONO_2$]/[HCl].

Motivated by evidence of a somewhat related minor channel reaction 2b

$$ClO + HO_2 \rightarrow HOCl + O_2 \quad (2a)$$

$$\rightarrow HCl + O_3 \quad (2b)$$

with a branching ratio of about 0.03 at low temperatures,[21] we repeated our sensitivity analysis after including reaction 2b. Results at 40 km show that [ClO]/[HCl] and [$ClONO_2$]/[HCl] are about 6 times more sensitive to reaction 1b with a 7% HCl yield than to reaction 2b with a 3% yield. However, at 30 km (1b) and (2b) have concentration ratio sensitivities that are large and comparable. Therefore, a minor yield for (2b) will impact mid-stratospheric chlorine partitioning, and improved branching yield measurements would be useful.

Finally, sensitivities for [$O_3$] from the same SENKIN outputs were similarly combined with the appropriate kinetics error bars to examine problems in the upper stratospheric ozone budget. At 40 km and 32°N vernal equinox, the [$O_3$] sensitivity to (1b) is −0.04; i.e., increasing the rate constant by the JPL-94 1$\sigma$ error bar will decrease [$O_3$] by 4%. This could be sufficient to bring the local ozone production and loss rates in the model into balance by reducing [ClO],[9] but it only partially accounts for the 2-D model prediction of 15−20% less [$O_3$] than observed.[2] Figure 2b identifies the rate constants for which improved measurement may help resolve the latter discrepancy and shows that the 22% net rms uncertainty for [$O_3$] is similar to the modeling discrepancy.

To examine the latitudinal and seasonal responses of upper stratospheric [$O_3$] to reaction 1b, we performed sensitivity calculations for other LLNL-2D boxes. At 42°S and 44 km, the inclusion of a 7% branch for (1b) increases [$O_3$] in June ($S_{1b}$ = 0.11) and December ($S_{1b}$ = 0.034) by 15% and 4%, respectively. This larger response of upper stratospheric [$O_3$] to (1b) in winter than in summer agrees with results given in Figure 1 of Chandra et al.[10] Reaction 1b is more effective in increasing upper stratospheric [$O_3$] at higher latitudes (42°) in winter than in summer, because of the increased importance of chlorine chemistry in colder regimes. However, recent 2-D model simulations underestimate upper stratospheric [$O_3$] by the largest amounts at lower latitudes (∼32°),[3] and our sensitivities show that the inclusion of reaction 1b is not sufficient to resolve this discrepancy.

### OH + ClO Reaction Mechanism and Rate Calculations

In this section reaction 1 is explored using methods of electronic structure and statistical reaction rate theories. The parameters used in our multichannel RRKM calculations[22] are given in Table 1. Reaction 1 can be described as a chemical activation process proceeding through an excited HOOCl* complex, which is shown schematically by the potential energy surface of Figure 3, where each transition state (TS) considered is labeled. The energized complex formed from OH + ClO collisions can redissociate to reactants (via TS1), proceed to $HO_2$ + Cl products (via TS2), dissociate over a barrier (TS3) to HCl + $O_2$, or be collisionally stabilized to form HOOCl. The formation of singlet HOOCl thus provides another channel for reaction 1

$$OH + ClO + M \rightarrow HOOCl + M \quad (1c)$$

**TABLE 1: Parameters for the RRKM Calculations**[a]

| | parameter | OH + ClO | OD + ClO |
|---|---|---|---|
| XOOCl | $\Delta H_f(0)$ | 1.57 | 0.41 |
| | $I$ | 84.0, 92.9, 10.5 | 87.6, 96.1, 11.6 |
| | $\nu$ | 3589, 1372, 851, 610, 407, 353 | 2615, 1013, 850, 609, 361, 292 |
| XO−OCl TS1 | $\Delta H_f(0)$ | 33.32 | 32.88 |
| | $I^+_{ad}$ (2D) | 609 | 633 |
| | $I_{int}$ | 0.91, 26.8, 0.3 × 0.91, 0.3 × 26.8 | 1.72, 26.8, 0.3 × 1.72, 0.3 × 26.8 |
| | $\nu$ | 3570, 843 | 2633, 843 |
| XOO−Cl TS2 | $\Delta H_f(0)$ | 32.29 | 31.43 |
| | $I^+_{ad}$ (2D) | 609 | 633 |
| | $I_{int}$ | 0.83, 0.3 × 15.52 (2) | 1.52, 0.3 × 16.73 (2) |
| | $\nu$ | 3436, 1392, 1098 | 2549, 1120, 1020 |
| XCl−$O_2$ TS3 | $\Delta H_f(0)$ | 31 ± 3 | 30 ± 3 |
| | $I$ | 13.9, 121, 135 | 15.1, 122, 136 |
| | $\nu$ | 3154, 1494, 972, 443, 189, rc [913i] | 2299, 1129, 928, 396, 185, rc [755i] |
| XCl + $O_2(^1\Delta)$ | $\Delta H_f(0)$ | 0.52 | 0.28 |

[a] Units: $\Delta H_f(0)$ in kcal/mol, $I$ in amu Å, and $\nu$ in $cm^{-1}$.

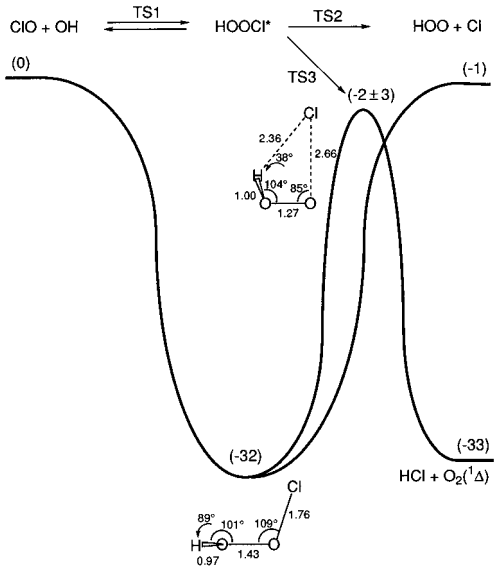


**Figure 3.** Potential energy surface (at 0 K) for the RRKM analysis of the OH + ClO reaction. Ab initio optimized geometries (distances in Å) for HOOCl and the HCl elimination transition state are shown as insets, with relative energies (kcal/mol) given in parentheses. The relative energy ($\Delta H(0)$) of the HCl elimination transition state was varied between 0.7 and −5.3 kcal/mol.

the possible atmospheric significance of which has been previously discussed.[23] The overall kinetics and branching are determined by the competition among channels 1a−1c and can be calculated from the transition-state and complex parameters, assuming energy is randomly distributed among the vibrational modes of the complex. In accordance with spin conservation, we have specified the products of (1b) as HCl($^1\Sigma^+$) + $O_2(^1\Delta)$ and note that the observation of (closed-shell) singlet metastable $O_2(^1\Delta)$ would help validate the mechanism outlined above. Production of ground-state triplet $O_2(^3\Sigma^-)$ would require a low probability intersystem crossing, and a noticeable HCl yield would then require that TS3 lie unrealistically low in energy. Note that our approach is similar to that used by Mozurkewich[24] to study reaction 2.

Our strategy is to use existing rate data to fix the parameters for TS1 and TS2 and to rely on ab initio calculations for the complex and TS3. The JPL-94 recommendation[12] for reaction 1 at 298 K is (1.7 ± 0.85) × $10^{-11}$ $cm^3$ $molecule^{-1}$ $s^{-1}$. Lipson et al.[1] report a value of (1.46 ± 0.23) × $10^{-11}$, but a recent measurement by Kegley-Owen et al.[25] gives a larger rate constant, 2.7 × $10^{-11}$. The rate constant determined by Lee and Howard[26] for reaction −1a is (9.1 ± 1.5) × $10^{-12}$ $cm^3$ $molecule^{-1}$ $s^{-1}$, although JPL-94 recommends much larger error bars based on scatter in other results. To compute rate constants for reactions 1 and −1a from the RRKM calculations, thermochemical data (including spin−orbit state energies) are needed for OH + ClO and Cl + $HO_2$. Data for OH and Cl were taken from the JANAF tables,[27] the $HO_2$ enthalpy of Hills and Howard[15] was adopted, and the ClO data are from NIST.[28] The equilibrium constant for reaction 1a, $K_{1a}(298) = 0.28$, is about half that derived from the ratio of the recommended rate constants. This suggests some error in the enthalpies or kinetics, perhaps supporting the larger value for $k_1$, and leaves some ambiguity in fitting the TS1 and TS2 parameters. The rms enthalpy uncertainty leads to over a factor of 2 uncertainty in $K_{1a}$.

The entrance transition states (via (1c) and (−1a)), corresponding respectively to TS1 and TS2, are radical−radical configurations that likely have insignificant electronic energy barriers. These loose transition states are readily described using the fragment vibrational modes, with the appropriate fragment rotational degrees of freedom treated as hindered internal rotations, as parametrized in the restricted Gorin transition-state model.[29] Rotational properties of the $HO_2$, OH, and ClO fragments were therefore used in computing the cone of acceptance for attractive orientations. The two largest $HO_2$ moments of inertia, and one each for OH and ClO, which are hindered by the presence of the other fragment in the transition states, are scaled by a hindrance factor $(1 - \eta)$ to account for this reduction in available phase space. The interfragment separation is used as the reaction coordinate, and the ratio of the perpendicular, adiabatic moments of inertia is given by $I^+_{ad}/I = (6D_0/RT)^{1/3} = 6.9$, where the bond dissociation energy of the complex ($D_0$) is approximately 32 kcal/mol (Table 1). Although different hindrance factors could be used for TS1 and TS2, we have chosen a single empirical value of $\eta = 0.7$, which results in rate constants that differ somewhat from the actual JPL-94 values[12] but are still well within the recommended error bars ($k_{1a}$ is 14% above $k_1$(JPL), while $k_{-1a}$ is underestimated by 11%). The predicted negative temperature dependence from this approach ($E_a/R = -95$ K) also agrees with the JPL-94 recommendations. In addition, only a minor (<5%) H/D isotope effect is predicted for (1a).

The various parameters required for HOOCl and the four-center TS3 were taken from calculations based on ab initio molecular orbital theory[30] and on density functional theory (DFT)[31] for comparison. The calculations treat electron correlation using various theoretical methods[32−38] and use correlation consistent polarized valence *N*-zeta basis sets (cc-pV*N*Z), $N$ = double, triple, or quadruple.[39] For optimizing the geometrical structures, the cc-pVDZ basis set as well as its augmented version (aug-cc-pVDZ)[39] was used at the QCISD (quadratic configuration interaction with single and double excitations) level,[32] while the force constant matrixes were calculated at QCISD/cc-pVDZ and at DFT[B-LYP]/aug-cc-pVDZ. The computations were performed using the MOLPRO[40] and G94[41] programs. The calculated geometries and vibrational frequencies for HOOCl and for TS3 are summarized in Figure 3 and Table 1. We have empirically scaled all of the QCISD harmonic vibrational frequencies by a factor of 0.96 for the RRKM calculations,[42] and it is these scaled values that are reported in Table 1. This level of theory provides suf-

**TABLE 2: TS3 Electronic Energy Barriers (kcal/mol)**

| method\basis set | cc-pVDZ | cc-pVTZ | cc-pVQZ |
|---|---|---|---|
| CASSCF[a] | 19.7 | 24.3 | 24.7 |
| DFT[B-LYP][b] | 29.9 | 34.0 | 34.7 |
| QCISD(T) | 27.3 | 33.5 | 34.8 |
| MRCISD[c] | 22.5 | 28.3 | 29.5 |
| MRCISD+SCC[d] | 23.1 | 29.2 | 30.6 |

[a] Full valence (20 electrons in 13 orbitals) active space. See refs 33 and 34. [b] Becke's 1988 gradient corrected exchange functional (ref 37) with the correlation functional of Lee, Yang, and Parr (ref 38). [c] Fourteen leading reference configurations taken from 14 electrons in 10 orbitals CASSCFs. See ref 36. [d] Pople type (ref 35) multireference size consistency corrections.

ficiently reliable parameters for the complex and TS3 to use in the RRKM calculations, and full details will be provided elsewhere.[42] The 0 K heat of formation of HOOCl (1.6 kcal/mol) was determined semiempirically, using its G2(QCI)[43] atomization energy. The physical properties of HOOCl are in agreement with other calculations[23] and bond additivity considerations,[44] which give 0 K formation enthalpies of 1.5 and 2.3 kcal/mol, respectively.

The four-center TS3, which was located after a comprehensive search and then verified, is reported here for the first time. TS3 is very asymmetric, with the OCl bond extended by ~50%, while the HO bond is stretched by only ~2.5%. The "late O−Cl" and "early H−O" nature of TS3 arises because the HO bond is much stronger than the OCl bond in HOOCl. The incipient HCl bond distance in TS3 is reduced by about 20% from that in HOOCl, mainly because of the decreases in the torsional angle (from 89° to 38°), the OOCl bond angle (from 109° to 85°), and the OO bond length (from 1.43 to 1.27 Å). Consequently, the reaction coordinate is a combination of many internal coordinate changes but is perhaps more closely associated with the torsional normal coordinate.

Most previous RRKM studies[45,46] of the isoelectronic reaction 3,

$$C_2H_5Cl \rightarrow HCl + C_2H_4 \qquad (3)$$

which is mechanistically analogous to (1b), have instead used vibrational normal mode coordinates corresponding to the C−Cl stretch, the C−H stretch, or the appropriate H−C−C bend as reaction coordinates. However, ab initio calculations[42,46] show that the transition state for HCl elimination from ethyl chloride is similar to TS3, i.e., very asymmetric with a nearly dissociated chlorine atom. Also, Jonas and Heydtmann[47] have used the out-of-plane deformation normal coordinate as the ethyl chloride reaction coordinate. This choice has implications for calculations of the H/D isotope effect, as discussed below. The *A* factor for decomposition of HOOCl to HCl is $3 \times 10^{13}$ s$^{-1}$, which is close to the experimental value[45] for reaction 3. The *A* factors for the decomposition reactions via TS1 and TS2 ($2 \times 10^{16}$ and $1.3 \times 10^{15}$ s$^{-1}$, respectively) also seem reasonable.

Calculations of the electronic contribution to the TS3 barrier (i.e., $\Delta E_e = E_e(\text{TS3}) - E_e(\text{HOOCl})$) are shown in Table 2. Progressing to the right and downward respectively are computations with more complete basis sets and with more sophisticated electron correlation methods. Note that, like the associated reactant (HOOCl) and products (HCl and $O_2(^1\Delta)$), TS3 is a closed-shell singlet, and therefore spin contamination from states of higher spin multiplicity is not a problem. Using any of the theoretical methods, the effect of basis set enlargement is to increase the barrier. For the largest basis set used (cc-pVQZ), the calculated electronic barriers range from 25 to 35 kcal/mol. However, the multireference CISD value, partially corrected for size inconsistency, is likely to be the best estimate of the electronic barrier, as it includes the effects of dynamical and nondynamical electron correlation in the most balanced manner.

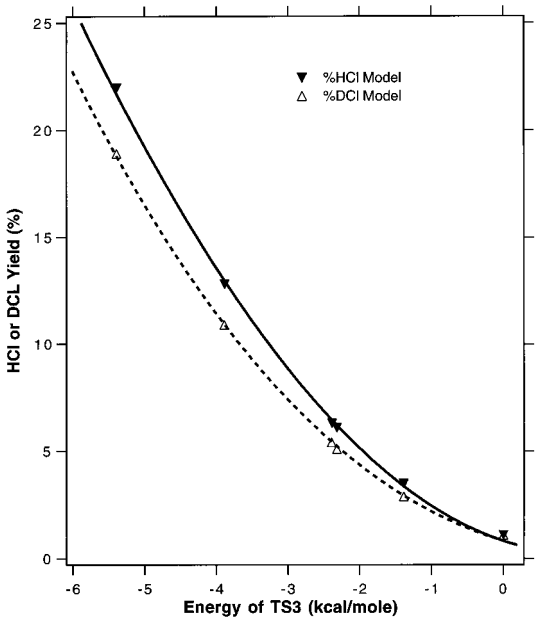


**Figure 4.** Branching fractions for the HCl and DCl products from the RRKM calculations of the reactions of OH and OD with ClO, as a function of the energy difference between the exit (TS3) and entrance (TS1) transition states. The abscissa uses the zero-point energy scale for the H system and has to be shifted by −0.54 kcal/mol for the D system.

Including the zero-point contributions puts TS3 29.3 kcal/mol above HOOCl, with an estimated uncertainty of ±3 kcal/mol (judging from the spread of values in Table 2 and, to a lesser extent, from analogous calculations[42] for reaction 3), which implies that TS3 lies 2.3 ± 3 kcal/mol below the entrance channel energy at 0 K. Given the likely uncertainty in the barrier height, we treat the energy ($\Delta H(0)$) of TS3 as a variable parameter in our RRKM model studies. The predicted $k_{1b}/(k_{1a} + k_{1b})$ or fractional HCl yield is plotted as a function of the TS3 relative energy in Figure 4. Between 220 and 300 K, the calculations have insignificant temperature dependence. A TS3 energy 2.5 kcal/mol below the TS1 entrance channel results in a 7% yield, the branching ratio being quite sensitive to this energy. The agreement between this experiment-driven rate theory energy and the ab initio value is encouraging. Computation of the transition-state barrier height with sufficient accuracy (±0.3 kcal/mol) to predict the branching ratio to two digits after the decimal is impractical, and other parameters such as the hindrance also contribute to the uncertainty, so accurate experimental values are necessary.

Because the branching fraction is a competition among TS1, TS2, and TS3 for the decomposition of the energized HOOCl, which in turn was formed through TS1, the yield vs energy curve in Figure 4 does depend somewhat on the hindrance parameter (i.e., *A* factor) choices made for TS1 and TS2. If, for example, we decide to increase the TS1 hindrance to exactly fit the JPL-94 $k_1$ value, or just to remove the use of equal hindrances, the predicted HCl branching fraction at a given energy would be increased, roughly by the fractional change in the *A* factor. Adjustments of enthalpy values would give similar effects. We also find that as the TS3 energy is lowered below the ab initio value, the overall rate constant $k_1$ begins to increase. At $\Delta H(0) = -5.3$ kcal/mol, $k_1$ is 27% larger.

It is interesting to compare the known barrier height for the isoelectronic ethyl chloride reaction 3 to that calculated for (1b). Viewing the reactions from the product (HCl addition) direction, the 29 kcal/mol barrier needed for a 7% (1b) branch is lower than the experimental barrier of 40 kcal/mol for HCl addition to ethylene.[45] However, the respective barriers for HBr and HI addition to ethylene of 35 and 29 kcal/mol[45] are lower. Our comparative theoretical study of reaction 3, including a more detailed description and analysis of our calculations for (1), will be reported elsewhere.[42]

Since the first measurement of the branching ratio for (1b) was recently reported for the OD + ClO system,[1] we also applied our theoretical methods to the isotopically labeled system. The DOOCl and TS3 parameters were also taken from our electronic structure calculations, $DO_2$ and OD vibrational modes were used to describe TS1 and TS2, and the appropriate zero-point energy corrections were made (Table 1). Deuteration results in a lowering of the TS3 barrier by 0.54 kcal/mol with respect to the TS1 entrance channel, and the TS2 relative energy also drops. The predicted total rate constant for OD + ClO is only 4% lower than for OH + ClO, and the branching ratio to DCl is 0.84 times that for HCl, as shown in Figure 4. Using the recently measured DCl yield of 5 ± 2%[1] and Figure 4, a similar, slightly larger HCl yield is predicted. Our calculations also predict that, for stratospheric temperatures, the HCl and DCl yields are virtually temperature independent, in agreement with the recent observations.

Alternate formulations of TS1−TS3 are possible, but the results will be similar provided the energetics and *A* factors do not change appreciably. The ratio of HCl/DCl isotopic yields, however, is sensitive to the identity of the reaction coordinate. If the approximate reaction coordinate used for HCl elimination via TS3 is replaced by a higher frequency stretching or bending normal coordinate (in disagreement with the theoretical prediction), then the isotope effect from the zero-point energy difference becomes larger. For reaction 3, ethyl chloride decomposition, the measured DCl/HCl rate ratio is 0.42 at 750 K.[47,48] Using the parameters of Table 1, we predict the analogous ratio for (1) to be 0.73 at 750 K, a significantly different result. However, computations[42] for reaction 3, using parameters for ethyl chloride and its elimination transition state that were generated in the same way as those for HOOCl and TS2 (Table 1), predict a D/H kinetic isotope effect of 0.40 at 750 K. This is consistent with the experimental measurements and lends confidence to our prediction of a significantly smaller isotope effect for reaction 1b at atmospheric temperatures.

Finally, we use the RRKM computations to investigate the pressure dependence of the rate constants and the possible formation of HOOCl. Even at 1 atm (220 K), the rate constants for channels 1a and 1b each change by less than 0.4% from their low-pressure limit. The formation rate constants for HOOCl from OH + ClO and from $HO_2$ + Cl are calculated to be $1.3 \times 10^{-13}$ and $3.2 \times 10^{-13}$ cm$^3$ molecule$^{-1}$ s$^{-1}$, respectively, which are negligible fractions of the rate constants to bimolecular products ($2.1 \times 10^{-11}$ cm$^3$ molecule$^{-1}$ s$^{-1}$). Therefore, no measurable pressure dependence of the rate constants and no significant stabilization of HOOCl* are to be expected under atmospheric or laboratory flow-reactor conditions. The 35% increase in the rate constant at higher pressure (from 95 to 180 Torr) for the DCl channel reported by Lipson et al.[1] is in disagreement with our predictions. (These preliminary experiments were primarily used to diagnose any heterogeneous DCl production.) The predicted HOOCl rate constants are only slightly sensitive to reasonable variations in its energy and vibrational frequencies (Table 1), and the chemical activation results are insensitive to these parameters at low pressures.

## Conclusions

Sensitivity−uncertainty analyses of the LLNL-2D model output confirm that the minor branch to HCl product from the OH + ClO reaction is an important kinetic factor in determining the mid to upper stratospheric chlorine budget. However, a 7% HCl channel can only partially account for model underestimations of upper stratospheric [$O_3$] at lower latitudes (32°N); it is more effective in increasing [$O_3$] at higher latitudes in winter (42°S in June). Other rate parameters were also identified that can influence the disagreements between models and observations. Using ab initio calculations of HOOCl and the four-center transition state for HCl elimination, we performed RRKM computations of the rate constants for the OH + ClO reaction as a function of HCl elimination barrier height, H/D isotopic substitution, temperature, and pressure. According to our calculations, only the first factor appears to be significant, and a barrier 2.5 kcal/mol below the reactants is consistent both with the uncertainty in the calculated barrier height and with the recent DCl measurements and also with the branching fraction proposed by atmospheric modelers. Measurements of the H/D isotope effect, pressure dependence, and $O_2(^1\Delta)$ are needed to confirm and refine the mechanism developed here using molecular orbital and RRKM theories.

**Acknowledgment.** The work at SRI was supported by the Atmospheric Chemistry Program of the U.S. Department of Energy. The work at UCI was supported by the Joan Irvine Smith and Athalie Clark Foundation and was also supported through an allocation of computer resources by the Office of Academic Computing. We thank Doug Kinnison and Peter Connell for providing the LLNL-2D model outputs and Dave Golden for his critical comments on the RRKM studies.

## References and Notes

(1) Lipson, J. B.; Elrod, M. J.; Beiderhase, T. W.; Molina, L. T.; Molina, M. J. *J. Chem. Soc., Faraday Trans.* **1997**, *93*, 2665.

(2) Albritton, D. A.; Watson, R. T.; Aucamp, P. J. *Scientific Assessment of Ozone Depletion: 1994*; World Metereological Organization: Geneva, Switzerland, 1996.

(3) Jackman, C. H.; Fleming, E. L.; Chandra, S.; Considine, D. B.; Rosenfield, J. E. *J. Geophys. Res.* **1996**, *101*, 28753.

(4) Solomon, S.; Portmann, R. W.; Garcia, R. R.; Thomason, L. W.; Poole, L. R.; McCormick, M. P. *J. Geophys. Res.* **1996**, *101*, 6713.

(5) McElroy, M. B.; Salawitch, R. J. *Science* **1989**, *243*, 763.

(6) Stachnik, R. A.; Hardy, J. C.; Tarsala, J. A.; Waters, J. W. *Geophys. Res. Lett.* **1992**, *19*, 1931.

(7) Michelsen, H. A.; Salawitch, R. J.; Gunson, M. R.; Aellig, C.; Kampfer, N.; Abbas, M. M.; Abrams, M. C.; Brown, T. L.; Chang, A. Y.; Goldman, A.; Irion, F. W.; Newchurch, M. J.; Rinsland, C. P.; Stiller, G. P.; Zander, R. *Geophys. Res. Lett.* **1996**, *23*, 2361.

(8) Toumi, R.; Bekki, S. *Geophys. Res. Lett.* **1993**, *20*, 2447.

(9) Jucks, K. W.; Johnson, D. G.; Chance, K. V.; Traub, W. A.; Salawitch, R. J.; Stachnik, R. A. *J. Geophys. Res.* **1996**, *101*, 28785.

(10) Chandra, S.; Jackman, C. H.; Douglass, A. R.; Fleming, E. L.; Considine, D. B. *Geophys. Res. Lett.* **1993**, *20*, 351.

(11) Lary, D. J.; Chipperfield, M. P.; Toumi, R. *J. Atmos. Chem.* **1995**, *21*, 61.

(12) DeMore, W. M.; Sander, S. P.; Golden, D. M.; Hampson, R. F.; Kurylo, M. J.; Howard, C. J.; Ravishankara, A. R.; Kolb, C. E.; Molina, M. J. Chemical Kinetics and Photochemical Data for Use in Stratospheric Modeling, Jet Propulsion Laboratory, 1994.

(13) Leu, M. T.; Lin, C. L. *Geophys. Res. Lett.* **1979**, *6*, 425.

(14) Burrows, J. P.; Wallington, T. J.; Wayne, R. P. *J. Chem. Soc., Faraday Trans. 2* **1984**, *80*, 957.

(15) Hills, A. J.; Howard, C. J. *J. Chem. Phys.* **1984**, *81*, 4458.

(16) Poulet, G.; Laverdet, G.; Le Bras, G. L. *J. Phys. Chem.* **1986**, *90*, 159.

(17) Wuebbles, D.; Connell, P.; Grant, K.; Kinnison, D.; Rotman, D. In *The Atmospheric Effects of Stratospheric Aircraft: Report of the 1992 Models and Measurements Workshop*; Prather, M. J., Remsberg, E. R., Eds.; NASA: Washington, DC, 1993; Vol I: NASA Refn. Pub. 1292.

(18) Dubey, M. K.; Smith, G. P.; Hartley, W. S.; Kinnison, D. E.; Connell, P. S. *Geophys. Res. Lett.* **1997**, *24*, 2737.

(19) Dubey, M. K.; Smith, G. P.; Kinnison, D. E.; Connell, P. S. Manuscript in preparation.

(20) Lutz, A. E.; Kee, R. J.; Miller, J. A. SENKIN: A Fortran Program for Predicting Homogeneous Gas-Phase Chemical Kinetics with Sensitivity Analysis, Sandia National Laboratories, 1988.

(21) Finkbeiner, M.; Crowley, J. N.; Horie, O.; Muller, R.; Moortgat, G. K.; Crutzen, P. J. *J. Phys. Chem.* **1995**, *99*, 16264.

(22) Larson, C. W.; Stewart, P. H.; Golden, D. M. *Int. J. Chem. Kinet.* **1988**, *20*, 27.

(23) (a) Francisco, J. S.; Sander, S. P.; Lee, T. J.; Rendell, A. P. *J. Phys. Chem.* **1994**, *98*, 5644. (b) Lee, T. J.; Rendell, A. P. *J. Phys. Chem.* **1993**, *97*, 6999.

(24) Mozurkewich, M. *J. Phys. Chem.* **1986**, *90*, 2216.

(25) Kegley-Owen, C. S.; Gilles, M. K.; Burkholder, J. B.; Ravishankara, A. R. 1997 Fall Meeting American Geophysical Union, poster A11B-22.

(26) Lee, Y.-P.; Howard, C. J. *J. Chem. Phys.* **1982**, *77*, 756.

(27) Chase, M. W., Jr.; Davies, C. A.; Downey, J. R., Jr.; Frurip, D. J.; McDonald, R. A.; Syverud, A. N. *J. Phys. Chem. Ref. Data* **1985**, *14* (Suppl. 1).

(28) Abramowitz, S.; Chase, M. W. *J. Pure Appl. Chem.* **1991**, *63*, 1449.

(29) Smith, G. P.; Golden, D. M. *Int. J. Chem. Kinet.* **1978**, *10*, 489.

(30) Hehre, W. J.; Radom, L.; Schleyer, P. v. R.; Pople, J. A. *Ab Initio Molecular Orbital Theory*; Wiley: New York, 1986.

(31) Parr, R. G.; Yang, W. *Density Functional Theory of Atoms and Molecules*; Clarendon Press: Oxford, 1989.

(32) Pople, J. A.; Head-Gordon, M.; Raghavachari, K. *J. Chem. Phys.* **1987**, *87*, 5968.

(33) Roos, B. O. *Adv. Chem. Phys.* **1987**, *69*, 399.

(34) (a) Werner, H.-J.; Knowles, P. J. *J. Chem. Phys.* **1985**, *82*, 5053. (b) Knowles, P. J.; Werner, H.-J. *Chem. Phys. Lett.* **1985**, *115*, 259.

(35) Pople, J. A.; Seeger, R.; Krishnan, R. *Int. J. Quantum Chem. Symp.* **1977**, *11*, 149.

(36) (a) Werner, H.-J.; Knowles, P. J. *J. Chem. Phys.* **1988**, *89*, 5803. (b) Knowles, P. J.; Werner, H.-J. *Chem. Phys. Lett.* **1988**, *145*, 514.

(37) Becke, A. D. *Phys. Rev. A* **1988**, *38*, 3098.

(38) Lee, C.; Yang, W.; Parr, R. G. *Phy. Rev. B* **1988**, *37*, 785.

(39) Woon, D. E.; Dunning, T. H. *J. Chem. Phys.* **1993**, *98*, 1358.

(40) Werner, H.-J.; Knowles, P. J., with contributions from Almlof, J.; Amos, R. D.; Deegan, M. J. O.; Elbert, S. T.; Hampel, C.; Lindh, R.; Meyer, W.; Peterson, K.; Pitzer, R.; Stone, A. J.; Taylor, P. R. MOLPRO, version 96.1.

(41) Frisch, M. J.; Trucks, G. W.; Schlegel, H. B.; Gill, P. M. W.; Johnson, B. G.; Robb, M. A.; Cheeseman, J. R.; Keith, T. A.; Petersson, G. A.; Montgomery, J. A.; Raghavachari, K.; Al-Laham, M. A.; Zakrzewski, V. G.; Ortiz, J. V.; Foresman, J. B.; Peng, C. Y.; Ayala, P. A.; Wong, M. W.; Andres, J. L.; Replogle, E. S.; Gomperts, R.; Martin, R. L.; Fox, D. J.; Binkley, J. S.; Defrees, D. J.; Baker, J.; Stewart, J. P.; Head-Gordon, M.; Gonzalez, C.; Pople, J. A. *GAUSSIAN 94*; Gaussian, Inc.: Pittsburgh, PA, 1995.

(42) McGrath, M. P.; Rowland, F. S. Manuscript in preparation.

(43) Curtiss, L. A.; Carpenter, J. E.; Raghavachari, K.; Pople, J. A. *J. Chem. Phys.* **1992**, *96*, 9030.

(44) Colussi, A. J.; Grela, M. A. *J. Phys. Chem.* **1993**, *97*, 3775.

(45) Benson, S. W.; Bose, A. N. *J. Chem. Phys.* **1963**, *39*, 3463.

(46) Toto, J. L.; Pritchard, G. O.; Kirtman, B. *J. Phys. Chem.* **1994**, *98*, 8359.

(47) Jonas, R.; Heydtmann, H. *Ber. Bunsen-Ges. Phys. Chem.* **1978**, *82*, 823.

(48) Blades, A. T.; Gilderson, P. W.; Wallbridge, M. G. H. *Can. J. Chem.* **1962**, *40*, 1526.